Validation of the pre-burn phase of advanced non-inductive operational scenario for tokamak-reactor in the high beta long pulse TCV experiments

I. Voitsekhovitch[1], S. Coda[2], C. Piron[3], F. Auriemma[4], R. Coosemans[2], O. Sauter[2], M. Vallar[2], M. Agostini[4], F. Bagnato[2], A. Burckhart[5], J. Decker[2], S. Garavaglia[6], A. Jardin[7], D. Mazon[8], A. Moro[6], S. Nowak[6], F. Orsitto[3], A. Pau[2], L. Piron[4], L. Simons[2], M. Ugoletti[4], V. Yanovskiy[9], and TCV Team[*]

[1]CCFE, Culham Science Centre, Abingdon, Oxon, OX14 3DB, UK; [2]Ecole Polytechnique Fédérale de Lausanne (EPFL), Swiss Plasma Center (SPC), CH-1015 Lausanne, Switzerland; [3]ENEA, Fusion and Nuclear Safety Department, C.R. Frascati, Via E. Fermi 45, 00044 Frascati (Roma) Italy; [4]Consorzio RFX-ISTP CNR, ENEA, INFN, Università di Padova, Acciaierie Venete SpA. I-35131 Padova, Italy; [5]Max-Planck-Institut fur Plasmaphysik, D85748 Garching, Germany; [6]ISTP-CNR, via R. Cozzi 53, 20125 Milano, Italy; [7]Institute of Nuclear Physics Polish Academy of Sciences (IFJ PAN), PL-31-342, Krakow, Poland, [8]CEA, IRFM, F-13108 Saint Paul Lez Durance, France; [9]Institute of Plasma Physics AS CR, Za Slovankou 1782/3, 182 00 Praha 8, Czech Republic

[*]*See author list of "H. Reimerdes et al 2022 Nucl. Fusion **62** 042018 (https://doi.org/10.1088/1741-4326/ac369b"*

I. Introduction

One of the possible optimisation strategies for the advanced non-inductive (NI) scenario for tokamak-reactor includes the formation of a reversed shear (RS) configuration and an Internal Transport Barrier (ITB) in the L-mode plasma and their sustainment during the L-H transition, density rise and burn phase. The plasma performance in the L-mode phase has been explored in recent TCV experiments where various RS configurations have been successfully produced during the combined electron cyclotron (EC) and neutral beam (NB) current drive (CD) phase at low density (n_e) and their evolution with n_e rise has been investigated [1, 2]. These advanced scenarios (ASs) are used here for the validation of a simple semi-empirical transport model which includes the stabilising effects of magnetic (s_m) and $E\times B$ (s_{ExB}) shear, validated previously in the broad range of RS configurations with thermal and particle ITBs on TFTR, DIII-D and JET [3]. The ASs developed at TCV extend the multi-machine ITB modelling database used in [3] towards the domain of dominant off-axis electron heating and negligible $E\times B$ shear and fast ion stabilisation of plasma transport, allowing one to isolate and estimate the stabilising effect of magnetic shear.

II. TCV advanced scenario database

Different strategies for producing a thermal electron ITB in RS configuration have been explored on TCV including: (a) the formation of a reversed q-profile in L-mode during the plasma current (I_{pl}) flattop by starting with a short low ECCD power (P_{ec}) step followed by the full ECCD power phase with NBCD power (P_{nbi}) added (Fig. 1); and (b) the formation of a RS configuration in NBI heated H-mode plasmas by adding ECCD after the L-H transition to combine the improved core and edge performance [1, 2]. This paper is focused on the analysis and modelling of the L-mode scenario. This scenario has been pursued both at fixed I_{pl} during the whole discharge duration (Fig.1, left) and by switching to zero loop voltage (V_{loop}) at/after the start of ECCD to maintain the plasma current non-inductively till the end of the discharge (Fig. 1, right). The performance of the RS plasmas has been extensively explored in a broad parameter space: I_{pl} = 0.12–0.16 MA, P_{ec} = 1.8-2.4 MW, P_{nbi} = 0.6-1.2 MW (slow and fast power ramp up rates have been tested) and line averaged densities n_{el} = (1.8-4.3)$\times 10^{19}$ m^{-3}, with the upper n_e limit determined by the X2 EC density cut-off. Consequently, a valuable database for the validation of integrated physics models (current diffusion, heating, and current drive (H&CD), fuelling, energy and particle transport) routinely applied in the reactor scenario simulations has been built.

III. Formation, sustainment and termination of reversed magnetic shear configurations

The analysis of the q-profile evolution is performed here for a selected set of representative discharges (Fig. 1) by using the ASTRA code [4] coupled to the stand-alone TORAY and KN1D codes and the internal self-consistently computed NCLASS and Fokker-Planck NBI modules, 1D kinetic neutral equation and SPIDER equilibrium code. The Thomson scattering measurements for the n_e and T_e profiles and the charge-exchange recombination spectroscopy (CXRS) measurements for the carbon density n_C and ion

temperature T_i are used in interpretative simulations. The data consistency test, particularly important for the validation of fast ion content, is performed by comparing (1) the W_{mhd} value computed by LIUQE equilibrium code and ASTRA and (2) the simulated and measured V_{loop} (for the discharges produced and simulated with prescribed I_{pl}) or I_{pl} (for the discharges produced and simulated with controlled V_{loop}). It is found that NI operation has been transiently achieved in many discharges, with a key contribution of the off-axis ECCD, important bootstrap (BS) current fraction and some NBCD (one example is shown on Fig. 2, top left panel). An elevated weakly reversed q-profile forms already at low ECCD power and then evolves to a strongly reversed shape during the combined ECCD+NBCD phase (Fig.2, top right). The duration of this NI phase is limited by a slow density increase (a small density pedestal forms at the start of ECCD in all analysed discharges and further develops during the combined H&CD phase performed at zero gas puff) leading to a reduction of T_e and ECCD efficiency (η_{ECCD}). The q-profile evolution in the final discharge phase occurs differently in scenarios with controlled I_{pl} and controlled V_{loop}. In discharge 77335 (I_{pl} control) the slow reduction of I_{EC} with n_e is compensated by an increase of the BS current (Fig.2, bottom left) with a similar current density profile alignment (Fig.2, bottom middle panels). Consequently, a stationary NI current as well as the RS configuration with weakly decreasing q_{min} (Fig.2, bottom right) are maintained till the end of the combined H&CD phase (during the last ~200 ms). In the discharges with V_{loop}=0 the ECCD reduction leads to a slow current ramp down (RD), increase of q_{min} and transition to a weakly reversed q profile. The RD phase appears to last longer in 76602 compared to 76606 and 76608. A second increase of I_{EC} around 1.5 s in 76602 correlates with the onset of MHD activity and the n_e reduction around mid-radius (EC absorption region) leading to the temporary increase of η_{ECCD}. The impact of the n_e rise on the sustainment of NI operation in 76602 is tested by simulating this discharge with the input data frozen at 1.2 s. A current hole configuration rapidly forms in this case due to the absence of central current, but a stationary fully NI operation is obtained with a small central current added (less than 10 kA). This extrapolation shows that the performed ASs are well optimised with presently available off-axis ECCD and NBCD TCV capabilities successfully approaching the fully NI steady state operational point.

IV. Modelling of energy and particle transport in the reversed shear plasmas

The magnetic shear effect on thermal and electron particle transport are investigated in predictive ASTRA simulations using the Bohm-gyroBohm (BgB) model with the magnetic and $E\times B$ shear multiplier (F_{shear}) included in the Bohm-like term [3]. The same plasma model as described in Section III with the continuity and ion and electron energy balance equations added is applied. The simulations start in the ohmic (OH) plasma at 0.3 s and continue till the end of the combined heating phase covering the whole plasma region ρ = 0-1. Time intervals with no/weak MHD activity (whenever possible) are selected for comparison with measurements. While the BgB model accurately predicts the thermal electron transport in the L-mode edge region in all simulated discharges due to its q^2 dependence increasing with radius, it is unable to reproduce the observed n_e pedestal build-up. For this reason, the edge particle diffusion coefficient is automatically adjusted to match the measured pedestal density, but the particle transport in all regions excluding the pedestal is still estimated with the L-mode version of the BgB model. With these assumptions the T_e and n_e profiles in the region with monotonic q are fairly accurately predicted in all simulated discharges (Figs. 3 and 4), with a small under-estimation around $\rho\approx$0.7 in some cases (i. e. close to the q=2 surface where the (2, 1) mode may still exist). A slightly off-axis n_e profile observed in the majority of performed ASs is not reproduced in modelling. Small particle ITBs are building in some cases (Fig. 3, top middle panel) following the bursts of the boundary neutral influx obtained with KN1D code. To eliminate the impact of the overestimated core n_e on the temperature prediction the simulations are performed also with the measured density (Fig. 4).

All performed simulations show that the core T_e achieved in experiments is clearly above its L-mode prediction by 10-26%. Such temperature increase is generally consistent with the transport reduction estimated with F_{shear}. In experiment and modelling a better core performance is achieved in the cases with larger EC power located at/inside $\rho(q_{min})$ (for example, at 1.08 s in 77335 (Fig. 4) and in 77606 and 77608

(Fig. 3)), although a strong reduction of thermal electron diffusivity in the RS region is obtained in all cases (an example is shown in Fig. 3 (bottom right)). A higher than predicted core T_e is observed in discharge 77335 after 1.4 s with strongly off-axis EC power absorption (Fig. 4, top left and right panels). Apart from the over-estimated transport, the discrepancy in the simulated and measured T_e may be explained by the penetration of the EC power into the centre due to EC waves scattering on the density fluctuations [5] or by the MHD reconnection bringing the fast electrons in the central region. The presence of MHD modes in the majority of discharges complicates the transport modelling interpretation. For example, a strong discrepancy between the measured and simulated T_e is obtained in 77335 at 1.08 s in presence of a strong n=1 mode (Fig. 4, top middle), leading to the loss of about 39% (2.9 kJ) of thermal electron energy W_e compared to the W_e value predicted with the BgB model. It should be added that it is difficult to validate accurately the shear effect on T_i in the absence of significant auxiliary ion heating. In these plasmas with a relatively small NBI absorption the ions are strongly decoupled with electrons and the central T_i about 0.3-0.8 keV is achieved that is consistent with the BgB model prediction and W_{mhd}.

V. Summary

A simple, computationally fast and well validated BgB model is frequently used for the development of reactor scenarios and estimation of fusion performance. The validation domain of this model with the magnetic shear term included is extended here towards the TCV advanced scenarios with off-axis ECCD and NBCD in L-mode plasmas with RS equilibria. The predicted n_e and T_e profiles are found to be close to the measured ones in the region with monotonic q in the absence of MHD events. The improvement of core thermal electron confinement as compared to the L-mode model prediction with no shear effects included (the simulated L-mode T_e is below the measured one by up to 26%) is found already with a small fraction of the EC power absorbed within $\rho(q_{min})$. Such improvement is compatible with prediction based on confinement enhancement through including the magnetic shear term in the BgB model. The magnetic shear stabilisation of anomalous transport can be further explored by applying X3 EC central heating in these RS plasmas and performing a heating power scan to test the ITB scaling with s_m. The validation of such transport model and, more generally, the integrated plasma model with strongly coupled parameters in future experiments provides a basis for the development of an advanced steady state scenario for a compact high magnetic field tokamak-reactor fully relying on EC and BS currents throughout the entire discharge and RS configuration with elevated q_{min} in the burn phase.

Acknowledgment. This work has been carried out within the framework of the EUROfusion Consortium, partially funded by the European Union via the Euratom Research and Training Programme (Grant Agreement No 101052200 — EUROfusion) and from the EPSRC [grant number EP/W006839/1]. To obtain further information on the data and models underlying this paper please contact PublicationsManager@ukaea.uk. The Swiss contribution to this work has been funded by the Swiss State Secretariat for Education, Research and Innovation (SERI). Views and opinions expressed are however those of the author(s) only and do not necessarily reflect those of the European Union, the European Commission or SERI. Neither the European Union nor the European Commission nor SERI can be held responsible for them. This work was supported in part by the Swiss National Science Foundation.

[1] C. Piron et al, 49th EPS Conf., July 3-8 2023, Bordeaux, France; [2] S. Coda et al, 29th IAEA FEC, October 16-21 2023, London, UK; [3] I. Voitsekhovitch et al, Phys. Plasmas **6**, 4229 (1999) and Czech. Journal of Physics **49** (1999) Suppl. S3, p. 41; [4] G. V. Pereverzev, P. N. Yushmanov, Report IPP 5/98 Max-Planck-Institute fur Plasmaphysik, 2002; E. Fable et al, Plasma Phys. Control. Fusion 55 (2013) 074007; [5] O. Chellai et al, Nucl. Fusion **61**, 066011 (2021)

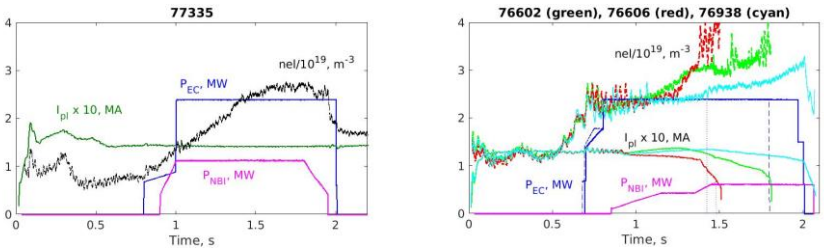

Fig.1. Plasma current, auxiliary powers and line averaged density in TCV advanced scenarios with controlled plasma current (77335, left) and V_{loop}=0 applied at 0.7 s (76602, 76606 and 76938, right). Discharge 76608 simulated in this paper has a similar scenario to 76606.

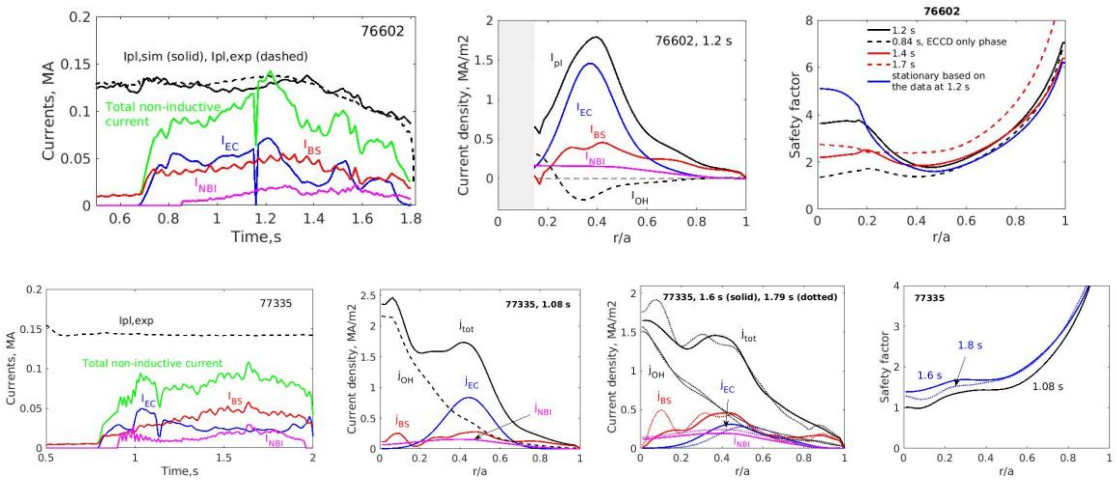

Fig.2. Total plasma and NI currents, current density and safety factor profiles obtained in interpretative simulations for 76602 performed with $V_{loop}=V_{loop,exp}$ (top) and 77335 performed with $I_{pl}=I_{pl,exp}$ (bottom). Steady-state safety factor profile achieved in predictive simulations with frozen input data in 76602 is shown by blue curve on the right top panel.

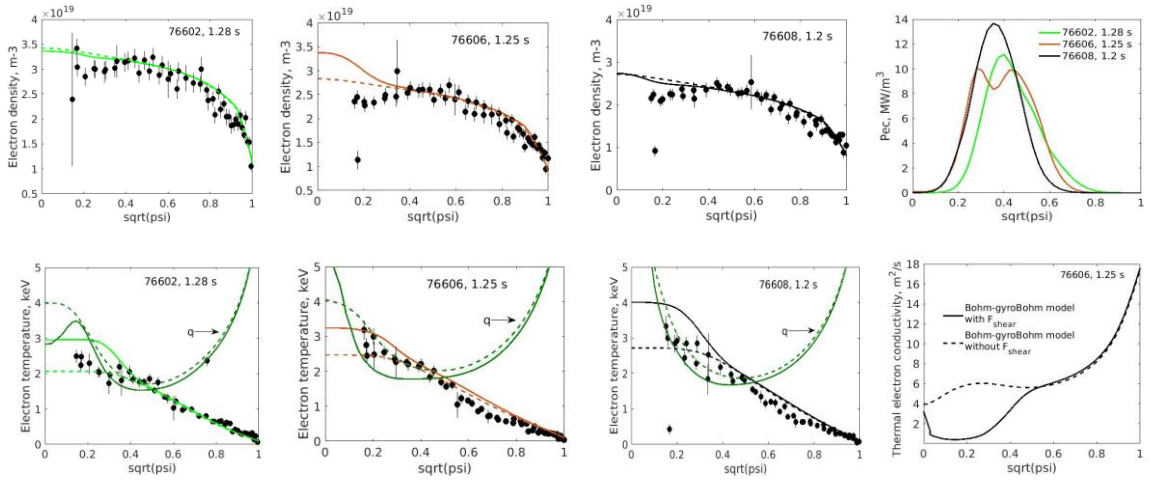

Fig. 3. Experimental (Thomson scattering data) and simulated n_e, T_e and q during the MHD-stable ECCD+NBCD phase in discharges with slightly different ECCD deposition (76602 and 76608) and with one gyrotron switched to heating mode (76606). The simulations performed with and without shear dependence in the BgB model are shown by solid and dashed curves correspondingly. EC power deposition profiles and an example of thermal electron diffusivity with and without shear dependence illustrating the effect of magnetic shear (76606) are shown in the right column.

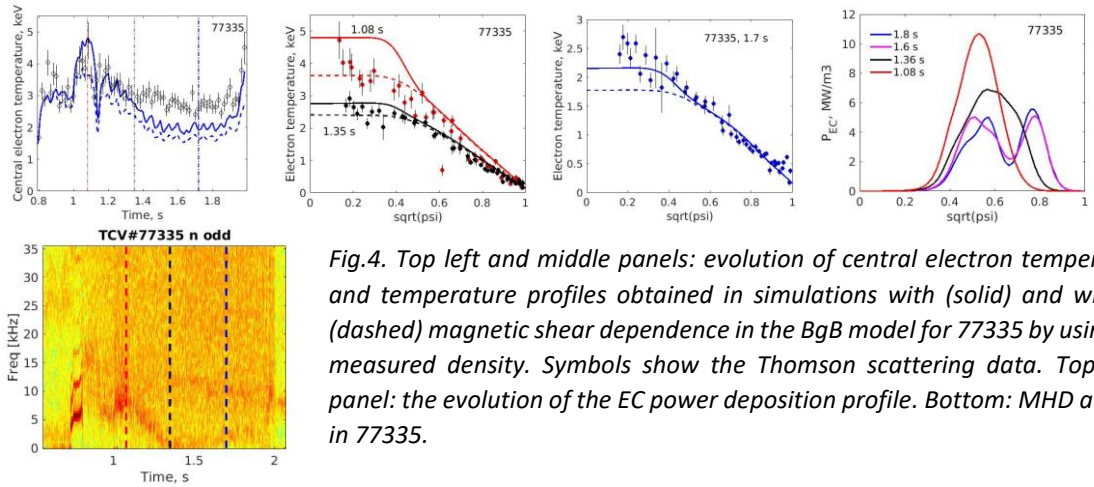

Fig.4. Top left and middle panels: evolution of central electron temperature and temperature profiles obtained in simulations with (solid) and without (dashed) magnetic shear dependence in the BgB model for 77335 by using the measured density. Symbols show the Thomson scattering data. Top right panel: the evolution of the EC power deposition profile. Bottom: MHD activity in 77335.